

COLOR SUPERCONDUCTIVITY IN QUARK STARS: POWERING GAMMA RAY BURSTS

RACHID OUYED¹ AND FRANCESCO SANNINO²
 NORDITA, Blegdamsvej 17 DK-2100 Copenhagen Ø, Denmark.
Draft version May 4, 2019

ABSTRACT

A two flavors color superconductive phase has been suggested as a plausible state of quark matter at high density. Here, we explore the possibility for such a state to exist at the surface of a quark star where temperatures below T_c (the critical temperature above which color superconductivity cannot exist) are first achieved following neutrino cooling. We develop a model which can quantitatively account for many of the observed features of gamma ray bursts. Among them, (i) the episodic activity of the engine (multiple and random shell emission); (ii) the two distinct categories of the bursts (~ 1 s and ~ 16 s duration); (iii) shell-shell collision dynamics and energetics ($0 < \Gamma_{shell} < 2 \times 10^5$ and $\rho_{shell} \propto \Gamma_{shell}^{-2}$); (iv) a peak duration vs energy dependence $t_p \propto E_p^{-0.5}$, and (v) gamma ray burst energy range, 8×10^{49} ergs $< E_{GRB} < 1.6 \times 10^{54}$ ergs. Our model, constrained by BATSE observations, favors $T_c \simeq 15$ MeV. We conclude that the superconductive gap is larger than 15 MeV for densities few times nuclear matter density. We establish a possible link between gamma ray bursts and color superconductivity. We show that bursts data can be used as a new tool to (a) derive the Mass-Radius plane for quark stars and (b) map the Quantum-Chromodynamics phase diagram in a regime impossible with current earth-based facilities.

Subject headings: dense matter – color superconductivity – stars: compact – stars: Gamma ray bursts

1. INTRODUCTION

Gamma-ray bursts (GRBs) were first discovered in the late 1960s by satellites watching for nuclear weapons tests in space. These bursts of γ -rays (the highest part of the electro-magnetic spectrum) were found to originate from the deepest confines of space near the outer reaches of the observable universe (on the order of 3 billion to 10 billion light-years away). Every day these powerful explosions illuminate the sky, coming from apparently random directions. They are the most short-lived energetic events in the universe, flashing and fading in a matter of seconds. They pass too quickly to aim a telescope for follow-up observations and one can only listen to the echo, the so-called afterglow (the X-ray and optical fading parts of the main burst). GRBs come in a great variety. Some bursts show spasms of intense radiation, with no detectable emission in between, whereas others are continuous, while the electro-magnetic emission spectra are complicated (Kouveliotou, Briggs & Fishman, 1995; Kulkarni et al. 1999; Piran 1999a; Piran 1999b).

A central problem contributing to the GRBs mystery is the unknown nature of the engine powering them. Many have been suggested (in the hundreds) but it is fair to say that we are still far from a definite answer. Regardless of the nature of the engine, however, it is widely accepted that the most conventional interpretation of the observed GRBs result from the conversion of the kinetic energy of ultra-relativistic particles to radiation in an optically thin region. The particles being accelerated by a fireball mechanism (or explosion of radiation) taking place near the central engine (Goodman 1986; Shemi & Piran 1990; Paczyński 1990).

The first challenge is to conceive of circumstances that would create a sufficiently energetic fireball. Many imaginative models involving for example black holes (Blandford & Znajek 1977), coalescing neutron stars (Ruffert & Janka 1999; Janka et al. 1999), conversion of neutron stars to quark stars (Olinto 1987; Cheng & Dai 1998; Bombaci & Datta 2000) have been suggested as a source for a fireball. While they can account for some aspects of GRBs, many of the important features remain un-explained such as their high energies (characterized by emission of photons of a few hundred keV), their high spectral and temporal variability (observed durations vary from several milliseconds to several thousand of seconds) (Kouveliotou, Briggs & Fishman 1995; Piran 1999a). A common denominator to the above mentioned models is the compact object element (Shapiro & Teukolsky 1983). Probably from the astrophysical point of view, the impasse stems from the poor understanding of the physics of such objects. The possibility of the onset of a newly revived state of quark matter - called color superconductivity - in these objects provides a different way to tackle the puzzle.

Quark matter at very high density is expected to behave as a color superconductor (Barrois 1977; Bailin & Love 1984). Recent work had lead to a renewed interest on the subject (Alford, Rajagopal & Wilczek 1998; Rapp et al. 1998; Rajagopal & Wilczek 2000a). This phase is characterized by its gap energy (Δ) associated to quark-quark pairing. As in ordinary superconductors, there exist a critical temperature (T_c) above which thermal fluctuations will wash out the superconductive state. A novel feature is the possible generation of light (with respect to the gap) glueball like particles in a two-flavor color super-

¹ ouyed@nordita.dk

² francesco.sannino@nbi.dk

conductive phase (often referred to as 2SC). This feature is a direct consequence of recent claims on global properties of 2SC (Rischke, Son & Stephanov 2000). These glueballs are made out of only three of the eight standard gluons, and are expected to quickly decay into photons. We demonstrate that if a 2SC state exists at the “surface” of a quark star not only do we provide a mechanism for a fireball generation but naturally account for many of the GRBs observed features.

The paper is presented as follows: §2 is devoted to the discussion of color superconductivity. In §3, we describe features of quark stars as compared to the more traditional gravitationally bound stars. The existence/formation of a superconducting phase in the surface layers of quark stars is discussed. We then explore the consequences of glueball formation and two-photon decay. In §4, we show how our model can power GRBs. We isolate two GRB regimes in §5 associated with small and massive quark stars. In §6, we show that variability is inherent to the inner engine nicely reproducing the internal shocks scenario. We summarize the model’s features and its predictions in §7. A discussion follows in §8 before concluding in §9.

2. COLOR SUPERCONDUCTIVITY

2.1. *QCD phase diagram*

QCD is fundamental in understanding matter at extreme conditions. Unfortunately, it is intractable in general, and consequently the QCD phase diagram (in the $\mu - T$ plane, where μ is the chemical potential simply related to matter density) is poorly known. Figure 1 is a schematic representation of a possible QCD phase diagram, among others that have been suggested (Rajagopal & Wilczek 2000a). At high temperature and density, matter is believed to be in a quark-gluon plasma phase (QGP). The hadronic phase lies in the region of low temperature and density where chiral symmetry is broken (via quark-antiquark pairs). At high densities but low temperatures, when nuclei melt into each other, it is now believed that a color superconductive phase sets in. Where and if, in the true QCD phase diagram, this transition occurs remains to be confirmed. Ultimately, lattice QCD results might shed some light on this issue but unlikely in the foreseeable future. The importance of mapping the QCD phase diagram has drawn wide interest as certainly is clear from the dedicated facilities, such as RHIC (Research on Heavy Ion Collision). While these facilities can only explore the regime of low density (although a wide range in temperature), astrophysics can, as we demonstrate in this paper, cover the high density and low temperature regime.

Color superconductivity is characterized by the formation of quark-quark condensate which carries a non-zero color charge unlike the quark-antiquark condensate of the hadronic phase. Hence in a superconductive phase, the color symmetry is spontaneously broken and a hierarchy of scales, for given chemical potential, is generated. Indicating with g the underlying coupling constant the relevant scales are: the chemical potential μ itself, the dynamically generated gluon mass $m_{\text{gluon}} \sim g\mu$ and the gap parameter (Son 1999) $\Delta \sim \mu e^{-\frac{1}{g}}$. Since for asymptotically high μ the coupling constant g (evaluated at the fixed scale μ) is $\ll 1$, we have:

$$\Delta \ll m_{\text{gluon}} \ll \mu . \quad (1)$$

The superconductive phase is divided into the 2-flavor and 3-flavor color superconductivity (2SC and CFL, respectively) depending on the number of light quarks in play. In the CFL case, the up, down and strange quarks ($N_f = 3$) are equally relevant while only the up and down ($N_f = 2$) ones are active in the 2SC case leading to fundamental differences between the two. Of relevance to the model of GRBs we develop in this work is the 2SC phase which we briefly discuss below (we refer the interested reader to Rajagopal & Wilczek 2000a for a review of the dynamical properties of 2SC, while for the low-energy effective theory see Casalbuoni, Duan & Sannino 2000).

2.2. *2SC and Light glueballs*

The superconductive phase for $N_f = 2$ does not break chiral symmetry and is characterized by five out of the eight gluons acquiring mass. The quarks up and down in the direction 3 of color remain massless (unless some new exotic type of condensate emerges) and are part of the relevant low energy excitations.

In Rischke, Son & Stephanov (2000), it has been shown that the relevant strong scale Λ'_{QCD} associated with the remaining unbroken but still confining $SU_c(2)$ gluodynamics can be related to the superconductive gap Δ via

$$\Lambda'_{QCD} \sim \Delta \exp\left(-\frac{a\mu}{g\Delta}\right) , \quad (2)$$

where g is the strong coupling constant and $a = 2\sqrt{2}\pi/11$. Eq(2) clearly indicates that at high densities Λ'_{QCD} is smaller than Δ . Here, we suggest that (as in ordinary QCD) this leads to additional $SU_c(2)$ type of light hadrons compared to the superconductive gap. These particles are made out of only three of the eight standard gluons referred to as light glueballs (LGBs). The maximum LGB mass is of the order of Λ'_{QCD} which is at most Δ .

2.3. *LGB properties*

The properties of LGBs relevant to our model (further properties are investigated in Ouyed & Sannino 2001) are:

i) The mass of the LGBs is fixed by Λ'_{QCD} and do not exceed Δ . Here, we actually take the LGB mass to be lighter than T_c .

ii) LGBs are color neutral with respect to the $SU_c(2)$ unbroken color group in the 2SC phase. The 2SC phase is a mixture of three components: (1) the LGBs, (2) the quark pairs, and (3) the remaining free up and down quarks.

iii) While ordinary glueballs are expected to decay into two-photons and other hadronic particles, LGBs will have the two-photon decay mode as the dominant one. We estimate a lower limit on the LGB lifetime to be of the order of 10^{-12} s by properly re-scaling ordinary glueballs properties to Λ'_{QCD} in the tens of MeV range (Gomm et al. 1986).

3. SUPERCONDUCTIVE QUARK STARS SURFACES

3.1. *Quark stars*

In Farhi & Jaffe (1984) words, quark matter can be seen as a Fermi gas of 3 quarks which together constitutes a color singlet baryon. It is useful to distinguish between two forms of quark matter: “strange matter” in which flavor

equilibrium has been established by the weak interactions; and “nonstrange quark matter” consisting only of u and d quarks. However, in these studies, having overlooked a possible phase transition at low temperature, the latter has been omitted. The onset and stability of any color superconductive phase is very sensitive to temperatures near the presently unspecified gap value (many different QCD models give a wide range of the gap value). In this paper, we focus on the possibility that some quark stars are born with temperatures just above T_c . We shall refer to these stars as “hot” quark stars (HQSs) in order to avoid any confusion with strange stars which are conjectured to exist even at zero pressure if strange matter is the absolute ground state of strong interacting matter rather than iron (Bodmer 1971; Witten 1984; Haensel, Zdunik & Schaefer 1986; Alcock, Farhi & Olinto 1986; Dey et al. 1998).

For illustration purposes, we borrow the language of the MIT-bag model formalism at low temperature and high density to describe HQSs (Farhi & Jaffe 1984). This gives a simple equation of state

$$P = b(\rho - \rho_{HQS})c^2, \quad (3)$$

where b is a constant of model-dependent value (close to, but generally not equal, to 1/3 of the MIT-bag model), and ρ_{HQS} is the density at zero-pressure (the star’s surface density). We should keep in mind that $T_c/\mu \ll 1$ as is confirmed later.

We assume that the features of HQSs (despite the settle differences pointed out above) are - to a leading order in T_c/μ - identical to that of strange stars. The latter have been studied in details. Of importance to our model (Alcock, Farhi & Olinto 1986; Glendenning & Weber 1992; Glendenning 1997):

i) The “surface” of a HQS is very different from the surface of a neutron star, or any other type of star. Because it is bound by the strong force, the density at the surface changes abruptly from zero to ρ_{HQS} . The abrupt change (the thickness of the quark surface) occurs within about 1 fm, which is a typical strong interaction length scale. The electrons being bound to the quark matter by the electro-magnetic interaction and not by the strong force, are able to move freely across the quark surface extending up to $\sim 10^3$ fm above the surface of the star. Associated with this electron layer is a strong electric field (5×10^{17} V/cm)- higher than the critical value (1.3×10^{16} V/cm) to make the vacuum region unstable to spontaneously create (e^+, e^-) pairs.

ii) The presence of normal matter (a crust made of ions) at the surface of the quark star is subject to the enormous electric dipole. The strong positive Coulomb barrier prevents atomic nuclei bound in the nuclear crust from coming into direct contact with the quark core. The crust is suspended above the vacuum region. One can show that the maximum mass of the crust cannot exceed $M_{crust} \simeq 10^{-5} M_\odot$ set by the requirement that if the density in the inner crust is above the neutron drip density ($\rho_{drip} \simeq 4.3 \times 10^{11}$ g/cc), free neutrons will gravitate to the surface of the HQS and be converted to quark matter. This is due to the fact that neutrons can easily penetrate the Coulomb barrier and are readily absorbed.

iii) HQSs can acquire masses (M_{HQS}) up to $2M_\odot$ with radii (R_{HQS}) up to 10 km. Unlike for neutron stars, which can only exists above a certain mass ($\sim 0.1M_\odot$), there is

no lower limit to the mass of the HQS. HQSs would be bound by the strong interaction even in the absence of gravity.

3.2. 2SC layer formation

The HQS is born with temperatures larger than T_c . Superconductivity is likely to first develop close to the surface where the temperature is the lowest. The HQS surface layer might enter the 2SC phase as illustrated in Figure 1. In the QCD phase diagram (Figure 2), (ρ_{B_0}, T_{B_0}) is the critical point beyond which one re-enters the QGP phase (the extent of the 2SC layer into the star). Other scenarios might involve a possible transition to a CFL phase beneath B_0 . While certainly interesting, they are not considered here (see discussion).

The portion of the star in 2SC is

$$M_{2SC} = \delta_{2SC} M_{HQS}, \quad (4)$$

where δ_{2SC} depends on the star’s mass.

It has been argued (Carter & Reddy 2000) that quark matter might cool slower when it becomes superconductive. A heuristic argument is that the neutrino emissivity is reduced by a factor (Schaab et al. 2000) of $e^{-\Delta/T}$ since the quarks are bound. This might suggests that the 2SC layer acts as a thermal insulator thus locking the star’s surface temperature at about the gap energy. This is not necessarily the case since, in this work, we isolate a mechanism where the 2SC state behaves as a heat regulator gradually cooling the star.

3.3. LGBs decay and photon thermalization

The photons from LGB decay are generated at energy $E_\gamma < T_c$ and find themselves immersed in a degenerate quark gas. They quickly gain energy via the inverse Compton process and become thermalized to T_c . We estimate the photon mean free path to be smaller than few hundred Fermi (Rybicki & Lightman 1979; Longair 1992) while the 2SC layer is measured in meters (see section on massive stars). A local thermodynamic equilibrium is thus reached with the photon luminosity given by that of a black body radiation,

$$L_\gamma = 3.23 \times 10^{52} \text{ ergs s}^{-1} \left(\frac{R_{HQS}}{5 \text{ km}} \right)^2 \left(\frac{T_c}{10 \text{ MeV}} \right)^4. \quad (5)$$

Note that independently of the mass of the glueballs, the photons will always be thermalized to T_c . While any photon generation mechanism in the surface of a quark star ought to lead to a similar picture, surprisingly enough we later show that 2SC turns out to be a natural working hypothesis (consolidating the LGB/photon process).

The energy for a single 2SC event is

$$\Delta E_{LGB} = \delta_{LGB} M_{2SC} c^2, \quad (6)$$

where δ_{LGB} is a constant (intrinsic property of 2SC) representing the portion of the 2SC that is in LGBs. The emission time is then

$$\Delta t_{cool} = \frac{\epsilon M_{HQS} c^2}{L_\gamma}, \quad (7)$$

with $\epsilon = \delta_{2SC} \delta_{LGB}$, and will be used later.

3.4. Episodic behavior

The star's surface density is reduced following photon emission. A heat and mass flux is thus triggered from the QGP phase to the 2SC layer re-heating and destroying the superconductive phase. The entire star is now above T_c and hence the cooling process can start again. This corresponds to the transition $[\rho(\mathbf{B}_0), T(\mathbf{B}_0)] \rightarrow [\rho_{HQS}, T(\mathbf{B}_0)]$ in the QCD phase diagram (thermal adjustment). The stage is now set for the 2SC/LGB/photon process to start all over again resulting in another emission. For the subsequent emission, however, we expect the system to evolve to point \mathbf{B}_1 generally located at different densities and temperatures than \mathbf{B}_0 . The cycle ends after N emissions when $\rho(\mathbf{B}_N) \simeq \rho_{HQS}$.

The time it takes for the whole star to be consumed by this process is

$$t_{engine} = \frac{M_{HQS} c^2}{L_\gamma} \simeq 1 \text{ s} \left(\frac{M_{HQS}}{M_\odot} \right) \left(\frac{5 \text{ km}}{R_{HQS}} \right)^2 \left(\frac{30 \text{ MeV}}{T_c} \right)^4, \quad (8)$$

which is representative of the engine's activity. The above assumes quick adjustment of the star following each event, but is not necessarily the case for the most massive stars.

4. POWERING GAMMA-RAY BURSTS

4.1. Fireball and baryon loading

The fireball stems from the LGB decay and photon thermalization. The photons are emitted from the star's surface into the vacuum region beneath the inner crust ($\sim 10^3$ fm in size). Photon-photon interaction occurs in a much longer time than the vacuum region crossing time. Also, the cross-section for the creation of pairs through interactions with the electrons in the vacuum region is negligible (Rybicki & Lightman 1979; Longair 1992). The fireball energy is thus directly deposited in the crust. If its energy density, aT_c^4 (with a being the radiation density constant), exceeds that of the gravitational energy density in the crust, energy outflow in the form of ions occurs. More specifically, it is the energy transfer from photons to electrons which drag the positively charged nuclei in the process. One can show that the condition

$$aT_c^4 > \frac{GM_{HQS}}{R_{HQS}} \rho_{crust}, \quad (9)$$

where ρ_{crust} is the crust density and G the gravitational constant, is equivalent to

$$\left(\frac{T_c}{30 \text{ Mev}} \right)^4 > \left(\frac{M_{HQS}}{M_\odot} \right) \left(\frac{5 \text{ km}}{R_{HQS}} \right) \left(\frac{\rho_{crust}}{\rho_{drip}} \right), \quad (10)$$

which is always true if $T_c > 30$ MeV. The fireball is thus loaded with nuclei present in the crust. Note that the 2SC layer is not carried away during the two-photon decay process because of the star's high gravitational energy density: $\rho_{HQS}/\rho_{drip} \gg 1$.

4.2. Multiple shell emission

The episodic behavior of the star together with the resulting loaded fireball (we call shell) offers a natural mechanism for multiple shell emission if $T_c < 30$ MeV. Indeed from eq(10) a higher T_c value would imply extraction of the entire crust in a single emission and no loading of the subsequent fireballs.

The fraction (f) of the crust extracted in a single event taking into account the condition $T_c < 30$ MeV is,

$$\Delta M_{crust} = f M_{crust}. \quad (11)$$

The shell is accelerated with the rest of the fireball converting most of the radiation energy into bulk kinetic energy. The corresponding Lorentz factor we estimate to be (Shemi & Piran 1990; Paczyński 1990),

$$\Gamma_{shell} \simeq \frac{\epsilon M_{HQS}}{f M_{crust}}, \quad (12)$$

where we used eq(6) and eq(11). ϵ and f depend on the star's mass and characterize the two emission regimes in our model.

5. MASSIVE VS LIGHT STARS: THE TWO REGIMES

When the inner crust density is the neutron drip value, one finds a minimum mass star of $\sim 0.015 M_\odot$. For masses above this critical value, the corresponding crusts are thin and light. They do not exceed few kilometers in thickness. Matter at the density of such crusts is a Coulomb lattice of iron and nickel all the way from the inner edge to the surface of the star (Baym, Pethick & Sutherland 1971). For masses below $0.015 M_\odot$, the crust can extend up to thousands of kilometers with densities much below the neutron drip. This allows us to identify two distinct emission regimes for a given T_c (< 30 MeV).

5.1. Light stars ($10^{-4} M_\odot < M_{HQS} < 0.015 M_\odot$)

These are objects whose average density is $\sim \rho_{HQS}$ ($M_{HQS} \simeq \frac{4\pi}{3} R_{HQS}^3 \rho_{HQS}$). The 2SC front extends deeper inside the star ($\delta_{2SC} \sim 1$). The star can be represented by a system close to \mathbf{A}_0 in Figures 2. Each of the few emissions (defined by ϵ) is thus capable of consuming a big portion of the star. Furthermore, the entire crust material can be extracted in a few 2SC/LGB/photon cycles ($\rho_{crust}/\rho_{drip} \ll 1$). Stars with mass less than $10^{-4} M_\odot$ have an associated crust mass which is too heavy ($M_{crust} > 5 \times 10^{-5} M_\odot$) for the *relativistic loaded fireball to occur* (which is the situation where the fireball energy is converted into bulk kinetic energy of the ions before it becomes thin. The $\Gamma > 100$ condition defines this regime and resolves the compactness problem) (Shemi & Piran 1990).

Using eq(8), the few emissions lead to

$$\begin{aligned} t_{tot} &\simeq \text{fraction} \times t_{engine} \\ &\simeq \text{fraction} \times 0.025 \text{ s} \left(\frac{M_{HQS}}{0.001 M_\odot} \right) \left(\frac{1 \text{ km}}{R_{HQS}} \right)^2 \left(\frac{30 \text{ MeV}}{T_c} \right)^4, \end{aligned} \quad (13)$$

where t_{tot} is representative of the observable time which takes into account the presence of the crust.

5.2. Massive stars ($M_{HQS} \geq 0.015 M_\odot$)

The surface density of a massive star being that of a light star (ρ_{HQS} given by $P = 0$ in eq(3)), defines a standard unit in our model. In other words, the mass of the 2SC layer in a massive star case is

$$\Delta M_{2SC,m} \simeq M_{2SC,l}, \quad (14)$$

where “ m ” and “ l ” stand for massive and light, respectively. It implies

$$\frac{\Delta R_{2SC,m}}{R_{2SC,m}} \simeq \frac{1}{3} \left(\frac{R_l}{R_m} \right)^3 \simeq \frac{1}{3} \left(\frac{1 \text{ km}}{5 \text{ km}} \right)^3 \simeq 0.003. \quad (15)$$

For a typical star of 5 km in radius, we then estimate a 2SC layer of about 15 meters thick (much larger than the photon mean free path thus justifying the local thermal equilibrium hypothesis). Equivalently,

$$\bar{\epsilon} = \frac{M_l}{M_m} \simeq \left(\frac{1 \text{ km}}{5 \text{ km}} \right)^3 \simeq 0.01, \quad (16)$$

where $\bar{\epsilon}$ is the average value. This naturally account for many events (or N fireballs). When the entire star is consumed it is of the order of

$$N \simeq \frac{1}{\bar{\epsilon}} \simeq 100. \quad (17)$$

Since most of the crust is at densities close to the neutron drip value, eq(10) implies that only a tiny part of the crust surface material (where $\rho_{crust} \ll \rho_{drip}$) can be extracted by each of the fireballs. This allows for a continuous loading of the fireballs.

The total observable time in our simplified approach is thus,

$$t_{tot} \simeq t_{engine} = 1 \text{ s} \left(\frac{M_{HQS}}{M_\odot} \right) \left(\frac{5 \text{ km}}{R_{HQS}} \right)^2 \left(\frac{30 \text{ MeV}}{T_c} \right)^4. \quad (18)$$

We isolated two regimes:

- (i) Light stars \Rightarrow short emissions.
- (ii) Massive stars \Rightarrow long emissions.

It appears, according to BATSE (Burst and Transient Source Experiment detector on the COMPTON-GRO satellite), that the bursts can be classified into two distinct categories: short (< 2 s) bursts and long (> 2 s, typically ~ 15 s) bursts. The black body behavior (T_c^4) inherent to our model puts stringent constraints on the value of T_c which best comply with these observations. Using $T_c \simeq 15$ MeV for illustration purposes, from eq(13) and eq(18) we obtain in the star’s rest frame

$$t_{tot} \simeq 16 \text{ s} \left(\frac{M_{HQS}}{M_\odot} \right) \left(\frac{5 \text{ km}}{R_{HQS}} \right)^2, \quad (19)$$

for massive stars (suggestive of long GRBs), and

$$t_{tot} \simeq 0.4 \text{ s} \left(\frac{M_{HQS}}{0.001 M_\odot} \right) \left(\frac{1 \text{ km}}{R_{HQS}} \right)^2, \quad (20)$$

for light stars (suggestive of short GRBs). There is a clear correlation (almost one to one) between the observed burst time and the time at which the source ejected the specific shell (see Figure 3 in Kobayashi, Piran & Sari 1997, for example). Note that $10 \text{ MeV} < T_c < 15 \text{ MeV}$ implies that only a portion of the crust is extracted. This is also consistent with our previous assumption ($T_c < 30 \text{ MeV}$) and subsequent calculations.

Eq(19) and eq(20) is simply eq(8) rescaled to the appropriate object size. We separated two regimes due to intrinsic differences in the engine and the crust. From the engine point of view, massive stars generate many more

emissions when compared to light ones, and no substantial reduction of the engine time is expected because of the omni-presence of the crust. Another important difference is related to the physics of the multiple re-adjustments following each event which is more pronounced for very massive stars. The latter among other factors is related to ϵ which can vary from one event to another.

6. SHELL-SHELL COLLISION

The Lorentz factor for the n^{th} shell is

$$\Gamma_{shell,n} = \frac{\epsilon_n M_{HQS,n}}{f_n M_{crust,n}} = \left(\frac{\epsilon_n}{\epsilon_{n-1}} \right) \left(\frac{f_{n-1}}{f_n} \right) \frac{(1 - \epsilon_{n-1})}{(1 - f_{n-1})} \Gamma_{shell,n-1}. \quad (21)$$

The ratio $\Gamma_{shell,n}/\Gamma_{shell,n-1}$ is a function of ϵ (which depends on the details of the cooling process and the spread of the 2SC front) and f (mostly related to the density in the crust). The two parameters should vary from one emission to another, and the ratio can be randomly greater or less than 1. As such, the shells will have random Lorentz factors and random energies. Faster shells will catch up with slower ones and will collide, converting some of their kinetic energy to internal energy.

Critical features of the shells are:

(i) When $T_c \simeq 15$ MeV, eq(10) gives $\rho_{crust}/\rho_{drip} \simeq 1/16$. For an appropriate crust density profile (using the equation of state given in Baym, Pethick & Sutherland 1971), from eq(11) we find $\bar{f} \simeq 0.01$. This implies

$$\Gamma_{shell} = 2 \times 10^5 \left(\frac{\epsilon}{0.01} \right) \left(\frac{0.01}{f} \right). \quad (22)$$

For massive stars then

$$0 < \Gamma_{shell} < 2 \times 10^5. \quad (23)$$

Note that a *relativistic loaded fireball* is not necessarily achieved since $\Gamma_{shell} < 100$ at times. Gaps in the GRBs spectra are thus expected according to our model.

(ii) Take a shell of thickness ΔX_{crust} to be extracted from the crust. The upper surface of the shell is extracted first while its lower surface lags behind by $(c - v_{shell})t \simeq ct/(2\Gamma_{shell}^2)$ (t is the time to eject the entire shell in the star’s rest frame). Taking into account mass conservation and the fact that $\Delta X_{shell} = 2\Gamma_{shell}^2 \Delta X_{crust}$, it is straightforward to show

$$\rho_{shell} \propto \frac{1}{\Gamma_{shell}^2}. \quad (24)$$

Interestingly enough, these are the exact features in the internal shock model which lead to the highest (up to 40%) conversion efficiency and the most desirable temporal structure (Kobayashi, Piran & Sari 1997; Mochkovitch, Maitia & Marques 1995).

For light stars, where both ϵ and f are close to unity, $\Gamma_{shell} \simeq 2 \times 10^5$. The shells are also heavier than in the massive stars case. We thus expect stronger shocks resulting in harder bursts. Combined with our previous results, this is suggestive of

- (i) Light stars \Rightarrow short and hard bursts.
- (ii) Massive stars \Rightarrow long and soft bursts.

7. FEATURES AND PREDICTIONS

7.1. GRB energies

The maximum available energy is when the heaviest HQS ($M_{HQS,max} \simeq 2M_{\odot}$) is entirely consumed. Since the lightest star in our model is $\sim 10^{-4}M_{\odot}$ we conclude that,

$$2 \times 10^{50} \text{ ergs} < E_{LGB} < 4 \times 10^{54} \text{ ergs}. \quad (25)$$

The corresponding GRB energy range is thus

$$8 \times 10^{49} \text{ ergs} < E_{GRB} < 1.6 \times 10^{54} \text{ ergs}, \quad (26)$$

where we used a fiducial conversion efficiency of 40%.

7.2. GRB total duration

From eq(19) and eq(20) we have

$$t_{tot} \simeq 16 \text{ s}, \quad (27)$$

for typical massive stars, and

$$t_{tot} \simeq 0.4 \text{ s}, \quad (28)$$

for typical light stars. The burst total duration does not exceed few seconds for light stars. Our estimate of the duration time for the massive star case should be taken as a lower limit. As we have said, a complete model should take into account star re-adjustments. Nevertheless, we can still account for a wide range in GRB duration by an appropriate choice of different values of the mass and radius.

7.3. Colliding iron shells

The fireball is loaded with heavy ions (iron and nickel) present in the HQS crust. This seems to fit recent claims of measured iron lines in some GRB observations (Antonelli et al. 2000). Further measurements might put our model to test.

7.4. Peak duration vs energy

The peak duration (t_p) is related to the time measured by a clock on the shell via (Fenimore & Ramirez-Ruiz 1999),

$$t_p \simeq \frac{t_{shell}}{2\Gamma_{shell}} = \frac{1}{2\Gamma_{shell}} \times \frac{\Delta X_{shell}}{c_s}, \quad (29)$$

where c_s is the speed of the shock front crossing the shell leading to the burst. We find

$$t_p \simeq \frac{1}{c_s} \times \frac{\epsilon M_{HQS}}{4\pi R_{HQS}^2 \rho_{crust}}. \quad (30)$$

In the above we used eq(12) and $M_{shell} = \Delta M_{crust} = 4\pi R_{crust}^2 \Delta X_{crust} \rho_{crust}$. The expression on the right is $\propto \Delta t_{cool}$ as can be seen from eq(7) and in our model is constant for a given star. c_s is the only parameter which is directly linked to the shell dynamics and energetics. Shock physics gives (Ouyed & Pudritz 1993)

$$c_s^2 \propto E_{int.}, \quad (31)$$

where $E_{int.}$ is the shell's internal energy gained during the collision observed as the peak's energy (E_p). That is,

$$t_p \propto E_p^{-0.5}, \quad (32)$$

in reasonable agreement with the power law dependence (index that is between -0.37 and -0.46) extracted from temporal vs energy structure in GRBs (Fenimore et al. 1995).

8. DISCUSSION

8.1. 2SC-II stars

The 2SC/LGB/photon process might proceed until one is left with an object made entirely of 2SC. We name such objects 2SC-II stars which are still bound by strong interactions due to the remaining 5 gluons used to gap/bind the quarks. They can be tiny enough ($M \sim 10^{-4}M_{\odot}$, $R \ll 1$ km) to be difficult to detect. BATSE observes on average one burst per day. This corresponds, with the simplest model to about once per million years in a galaxy (Piran 1999a). In the Milky way we thus expect about 10^4 of 2SC-II stars effectively hiding baryonic matter.

8.2. An alternative scenario

In principle, one can imagine a scenario where the CFL replaces the 2SC. A CFL is allowed if the gap is larger than the difference between the u (d) and s quark Fermi momenta (Rajagopal & Wilczek 2000a) (i.e., $\Delta > m_s^2/2\mu$ where m_s is a density dependent effective strange quark mass). For $m_s = 200 - 300$ MeV and $\mu = 400 - 500$ MeV (reasonable for compact stars), CFL would exists only if Δ is larger than about $40 - 110$ MeV. For lower values of the gap 2SC is the favored phase. Our derived value of $\Delta > 15$ MeV hints towards the 2SC picture while not ruling out CFL. However, we foresee many problems with the CFL. For example, there are supporting arguments that the CFL phase is electrically neutral, despite the unequal quark masses, and even in the presence of an electron chemical potential (Rajagopal & Wilczek 2000b). If true, it implies that a CFL transition at the surface of the star is either unlikely or positively charged particles must be generated to maintain electric neutrality. Further problems with CFL associated to the r -mode instability have been pointed out (Madsen 2000) although recently questioned due to the possibility of CFL crystallization (Alford, Bowers & Rajagopal 2000). In the eventuality of the resolution of the above mentioned problems and Δ is large enough, our model remains valid when replacing 2SC by CFL provided a source of photons is found (suggestive of the process $\pi^0 \rightarrow \gamma\gamma$).

8.3. The Mass vs Radius Plane

Our model constrained by GRBs data hints to $T_c \simeq 15$ MeV. Such a universal value is consistent with our assumed universal surface density (ρ_{HQS}) and seems to support the MIT bag model.

We suggest a way of plotting the Mass-Radius plane for quark stars using GRBs data. The burst total energy $E_{GRB} \simeq 0.4Mc^2$ gives us the mass while the burst total duration (t_{tot}) the radius. The Mass-Radius plane could be of great help when selecting the correct dense matter equation of state.

9. CONCLUSION

Perhaps the most exciting aspect of our model, if true, suggests that quark stars not only exist in nature but we see their signatures everyday (BATSE has been detecting one GRB per day for the last six years!). It is also suggestive of the onset of color superconductivity in very high dense media. We find that GRBs time duration can

be simply related to the superconductive critical temperature. Our model, constrained by BATSE observations, favors $T_c \simeq 15$ MeV. We conclude that the superconductive gap is larger than 15 MeV giving valuable information to constraint the QCD phase diagram.

10. ACKNOWLEDGMENTS

It is a pleasure for us to thank J. Schechter for interesting discussions.

REFERENCES

Alcock, C., Farhi, E., & Olinto, A. 1986, *ApJ*, 310, 261.
 Alford, M., Rajagopal, K., & Wilczek, F. 1998, *Phys. Lett. B*, 422, 247.
 Alford, M., Bowers, J., & Rajagopal, K. 2000, *hep-ph/0008208*.
 Antonelli, L. A. et al. 2000, *ApJ*, 545, L39.
 Bailin, D., & Love, A. 1984, *Phys. Rept.*, 107, 325.
 Barrois, B. 1977, *Nucl. Phys. B*, 129, 390.
 Baym, G., Pethick, C. J., & Sutherland, P. G. 1971, *ApJ*, 170, 299.
 Blandford, R. D., & Znajek, R. L. 1977, *MNRAS*, 179, 433.
 Bodmer, A. R. 1971, *Phys. Rev. D*, 4, 1601.
 Bombaci, I., & Datta, B. 2000, *ApJ*, 530, L69.
 Carter, G. W., & Reddy, S. 2000, *hep-ph/0005228*.
 Casalbuoni, R., Duan, Z., & Sannino, F. 2000, *Phys. Rev. D* **62**, 094004.
 Cheng, K. S., & Dai, Z. G. 1996, *Science*, 280, 407.
 Dey, M., Bombaci, I., Dey, J., Ray, S., & Samanta, B. C. 1998, *Phys. Lett. B*, 438, 123.
 Farhi, E., & Jaffe, R. L. 1984, *Phys. Rev. D*, 30, 2379.
 Fenimore, E. E. et al. 1995, *ApJ*, 448, L101.
 Fenimore, E. E., & Ramirez-Ruiz, E. 1999, in *Gamma-Ray Bursts: The first three minutes*, ASP Conference Series, Vol. 190, eds. J. Poutanen and R. Svensson, p67.
 Glendenning, N. K., & Weber, F. 1992, *ApJ*, 400, 647.
 Glendenning, N. K., *Compact stars* (Springer, 1997).
 Gomm, H., Jain, P., Johnson, R. & Schechter, J. 1986, *Phys. Rev. D*, 33, 801.
 Goodman, J., 1986, *ApJ*, 308, L47.
 Haensel, P., Zdunik, J. L., & Schaefer, R., 1986 *A&A*, 160, 121.
 Janka, H. -T., Eberl, T., Ruffert, M., & Fryer, C. 1999, *ApJ*, 527, L39.
 Kobayashi, S., Piran, T. & Sari, R. 1997, *ApJ*, 490, 92.
 Kouveliotou, C., Briggs, M. S., & Fishman, G. J., (Eds), *Gamma Ray Bursts*, AIP Conf. Proc., 384 (AIP, New York, 1995).
 Kulkarni, S. R., et al. 1999, *Nature*, 398, 389.
 Longair, M. S., *High energy astrophysics* (Cambridge Univ. Press, 1992).
 Madsen, J., 2000, *Phys. Rev. Lett.*, 85, 10.
 Mochkovitch, R., Maitia, V., & Marques, R. 1995, in *Towards the Source of Gamma-Ray Bursts*, Proceedings of 29th ESLAB Symposium, ed. K. Bennet & C. Winkler, 531.
 Olinto, A. 1987, *Phys. Lett. B*, 192, 71.
 Ouyed, R. & Pudritz, R. E. 1993, *ApJ*, 419, 255.
 Ouyed, R., & Sannino, F. 2000, in preparation.
 Paczynski, B. 1990, *ApJ*, 363, 218.
 Piran, T. 1999a, *Phys. Rev.*, 314, 575.
 Piran, T. 1999b, in *Gamma-Ray Bursts: The first three minutes*, ASP Conference Series, Vol. 190, eds. J. Poutanen and R. Svensson, p3.
 Rajagopal, K. & Wilczek, F. 2000a, *hep-ph/0011333*.
 Rajagopal, K. & Wilczek, F. 2000b, *hep-ph/0012029*.
 Rapp, R., Schäfer, T., Shuryak, E. V., & Velkovsky, M. 1998, *Phys. Rev. Lett.*, 81, 53.
 Rischke, D. H., Son, D. T., & Stephanov, M. A. 2000 *hep-ph/0011379*.
 Ruffert, M., & Janka, H. -T. 1999, *A&A*, 344, 573.
 Rybicki, G. B., & Lightman, A. P. *Radiative processes in astrophysics* (Wiley, 1979).
 Schaab, C., Hermann, B., Weber, F., & Manfred, K. 2000, *ApJ*, 480, L111.
 Shapiro, S. L., & Teukolsky, S. A. *Black holes, white dwarfs, and neutron stars: The physics of compact objects* (Wiley-Interscience, 1983).
 Shemi, A., & Piran, T. 1990, *ApJ*, 365, L55.
 Son, D. T., 1999, *Phys. Rev. D*, 59, 094019.
 Witten, E. 1984, *Phys. Rev. D*, 30, 272.

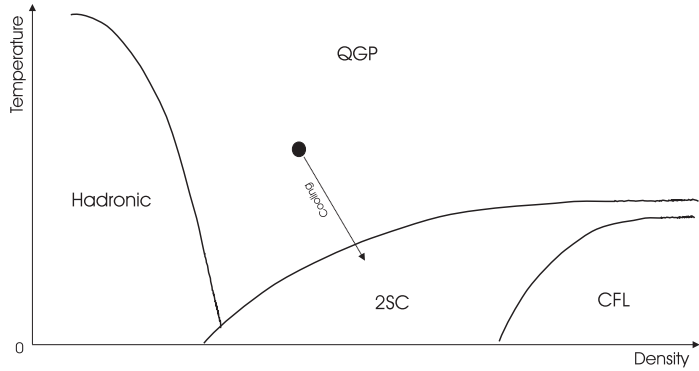


FIG. 1.— A schematic representation of a possible QCD phase diagram (Rajagopal & Wilczek 2000a). At high temperature and density, matter is believed to be in a quark-gluon plasma phase (QGP). The hadronic phase lies in the region of low temperature and density where chiral symmetry is broken via quark-antiquark pairs. At very high density but low temperature, when nuclei melt into each other, it has been suggested that a color superconductive phase might set in. 2SC denotes a 2-flavor color superconductive regime. CFL is the 3-flavor regime. The arrow depicts a plausible cooling path of a HQS surface leading to the onset of color superconductivity.

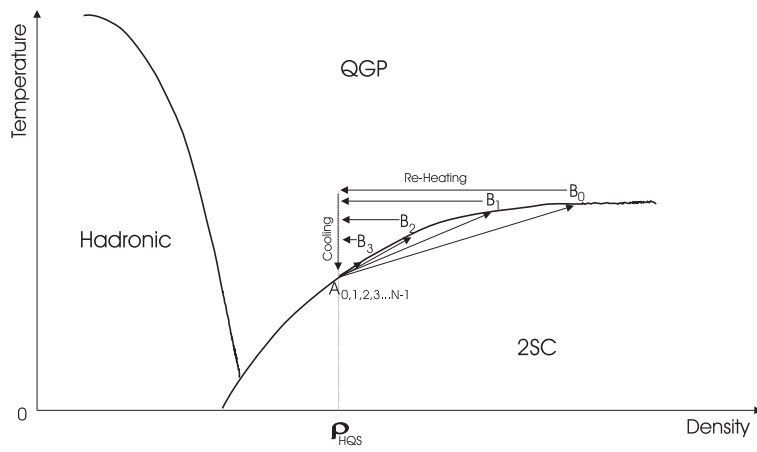


FIG. 2.— The episodic emission as illustrated in the QCD phase diagram. The 2SC front spreads deep inside the star and stops at B_0 before re-entering the QGP phase. Following photon cooling, heat flows from the core and re-heats the surface. The star then starts cooling until A_1 is reached at which point the stage is set for the 2SC/LGB/photon process to start all over again ($A_1 \rightarrow B_1$) resulting in another emission.